11th International Symposium on Turbulence and Shear Flow Phenomena (TSFP11)
Southampton, UK, July 30 to August 2, 2019

COUPLING DIRECT NUMERICAL SIMULATION WITH POPULATION BALANCE MODELLING FOR PREDICTING TURBULENT PARTICLE PRECIPITATION IN A T-MIXER

Hin Yan Tang
Department of Mechanical Engineering
Imperial College London
Exhibition Road, London SW7 2AS
hin.tang16@imperial.ac.uk

George Papadakis
Department of Aeronautics
Imperial College London
Exhibition Road, London SW7 2AS
g.papadakis@imperial.ac.uk

Stelios Rigopoulos
Department of Mechanical Engineering
Imperial College London
Exhibition Road, London SW7 2AS
s.rigopoulos@imperial.ac.uk

ABSTRACT

In this study we develop a methodology for predicting the particle size distribution (PSD) in particulate process, a process used for producing particulate materials, by coupling population balance modelling and direct numerical simulation. It is employed in investigating the turbulent precipitation of $BaSO_4$ in a T-mixer. The high resolution allowed us to capture the dominating mechanisms. Particle formation is most intense in the impingement and the reactant consumption in each precipitation mechanism depends on the mixing intensity. Different particle formation states and their characteristics on the PSD in the early stage are then identified. Comparison with an ideal reactor shows that the distribution can be controlled by altering the mixing environment.

INTRODUCTION

Precipitation refers to a particle formation process in which small particles are precipitated from the reaction between liquid phase ionic solutions. It generally consists of four mechanisms, namely nucleation, growth, aggregation and breakage. The particle size distribution (PSD) of the precipitated particles is of interest as it determines the quality of the particle products. Suitable mixing conditions are paramount to maximise the yield and selectivity and hence minimise the waste of materials due to insufficient or excessive mixing.

In the context of turbulent precipitation, the mixing of the flow field changes the global environment for the reaction and precipitation. When the hydrodynamics mixing timescales and the precipitation timescales are comparable, turbulence assumes an important role. The turbulent intensity can have significant effects on the supersaturation of the solution, a driving force of precipitation process, leading to a spatially inhomogeneous distribution. This make the evolution inside the reactor very comples. It is therefore vital to understand how the PSD can be controlled in the process such that the system can be tailored to specific application.

This project explores the effect of mixing on particulate process and the PSD using Direct Numerical Simulation (DNS) and Population Balance Modelling. The application of such DNS-PBE approach is demonstrated on a nanoparticle precipitation process in a T-mixer.

CASE STUDY

To demonstrate the application of the DNS-PBE approach, we simulate the experiment of Schwarzer & Peukert (2004a) and Schwarzer et al. (2006). In their work, they performed unseeded continuous precipitation of Barium Sulphate ($BaSO_4$) nanoparticles in a T-mixer. $BaSO_4$ particles were precipitated from mixing Barium Chloride ($BaCl_2$) and Sulphate acid (H_2SO_4) as indicated in Eq. (1).

$$BaCl_2 + H_2SO_4 \rightarrow BaSO_4 + 2 \cdot HCl \quad (1)$$

The T-mixer used consists of two 0.5mm diameter inlet pipes each 10 mm long and 1 mm width square cross-section mixing channel. Two jets of water containing $BaCl_2$ and H_2SO_4 are injected in each inlet respectively and turbulence is created at the impingement to enhance mixing. Laminar parabolic profile (Poiseuille flow) was assumed at the inlets. The setup is illustrated in Figure 1. In addition, the ion concentration at each inlet is tabulated in Table 1. Under this concentration, the Barium excess is high enough to suppress aggregation (Schwarzer & Peukert, 2004b), leaving the primary precipitation mechanisms as nucleation and growth only.

Table 1. Inlet Ion Concentration

Ion species	C_{inlet} [kmol/m^3]	Inlet
Ba^{2+}	0.5	1
Cl_2	1	1
H_2	0.66	2
SO_4^{2-}	0.33	2

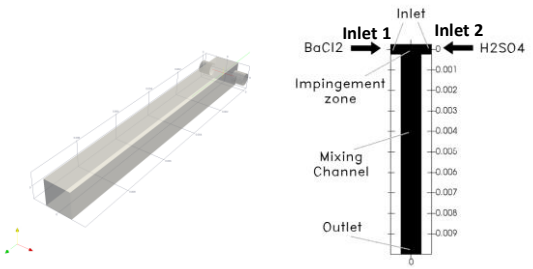

Figure 1. Illustration of the T-mixer

MODELLING

DNS-PBE Coupling

Several works have attempted to couple or include hydrodynamic effects in PBEs, for instance, the LES-PDF-PBE method (Sewerin & Rigopoulos, 2017) and the CFD coupled DQMOM method (Metzger & Kind, 2017). The use of DNS on hydrodynamics coupling with population dynamics has been investigated through moment methods and Lagrangian particle tracking (Gradl, et al, 2006; Schwarzer, et al, 2006), but the results are path dependent. In the current study, we coupled two in-house codes: Pantarhei and CPMOD, to solve the PSD directly at any point in the entire domain. The discretisation strategy is discussed below:

Direct Numerical Simulation

Since the size of the particles are small, we assumed that they and have no effects on the fluid properties. The flow field is therefore incompressible and Newtonian and is solved by our inhouse DNS code PANTARHEI (Immanuvel, et al., 2017). In the DNS, the Navier-Stokes equations are solved using the fractional step method with standard incremental pressure-correction scheme. Third-order backward difference scheme is used for time discretization (Fishpool & Leschziner, 2009). Only the orthogonal diffusion terms are treated implicitly while convection and non-orthogonal terms are treated in explicit manner with third-order extrapolation. The elements of the coefficient matrixes remain constant. As such, iterative velocity-pressure correction can be avoided at each time step.

Apart from the flow field, the transport of the scalar quantities is solved with DNS. This includes the ion species concentration as well as the PSD. Eq. (2) shows the transport equation for the ion species. We assumed Sc = 1 for all scalars. The discretisation strategy in the transport terms is similar to the momentum equations except the fact that it is solved fully explicitly. Special treatment is required on the reaction source term to ensure consistent consumption in the ion concentration and in the product PSD. This will be discussed in the next section.

$$\frac{\partial C_i}{\partial \mathrm{t}} + \boldsymbol{u} \cdot \nabla C_i = \frac{\mu}{\mathrm{Sc}} \nabla^2 C_i + r_i \tag{2}$$

The mesh used in the simulation is Cartesian with 21 million cells and is generated in ICEM. The mesh sizes can resolve up to Kolmogorov scale. A statistically independent flow field was achieved with 10 flow-through time before begin simulating the precipitation process.

Population Balance Modelling

The PSD can be described by a set of number densities where the particle size domain is discretised into intervals. Each number density represents the number of particles per unit volume that are within particular size interval. The number density used in this project is defined in volume basis as in Eq. (3). An exponential grid with 40 intervals is used to represent the particle size domain. The evolution of the number density is governed by a population balance equation (PBE). The transported PBE which includes the flow field effect is shown in Eq. (4).

Starting from the left, the terms in Eq. (4) represent the transient, convection, diffusion as well as the contribution from the nucleation and growth mechanisms respectively. It can be treated as a scalar transport equation where the nucleation and growth terms act as additional source terms in the transport equation. The source terms for the PBE is discretised with our in-house code CPMOD (Rigopoulos & Jones, 2003) based on finite volume method in particle size space whereas the transport effects are taken care by the DNS. A TVD scheme is implemented for the growth term discretisation (Qamar, et al., 2006) to ensure mass conservation in the flux through each size interval.

$$n_j = \frac{dN_j}{VdV} \tag{3}$$

$$\frac{\partial n_j}{\partial \mathrm{t}} + \boldsymbol{u} \cdot \nabla n_j = \frac{\mu}{\mathrm{Sc}} \nabla^2 n_j + B_0 \delta(L - L_{nuc}) - \frac{\partial G \cdot n_j}{\partial L} \tag{4}$$

In addition to the mass conservation in the particle size domain, the mass consumption in ions during reaction have to be conserved with the mass generation of particles. As they are governed by different equations (the ion concentration is governed by Eq. (2) while the particle number is governed by Eq. (4)), the source term in the ion transport should be consistent with that in the PBE. We compute the reaction source term in Eq. (2) by lumping the PBE source terms in all interval together as shown in Eq. (5). This ensures the first moment of distribution, which indicates the total particle volume in the PSD, is conserved. The source terms in reaction and PBE are thereby guaranteed to be consistent so long as they are discretised in the same manner.

$$r_j = \frac{M_w}{\rho} * \left[B_0 * V_{m,nuc} + \sum_{i=1}^{m} V_{m,i} * \left(\frac{\partial G \cdot n_i}{\partial V}\right)_i * n_i * dV_i\right] \tag{5}$$

In order to investigate the role of mixing in the process, the results are compared to an ideal Perfectly Stirred Reactor (PSR) case. It assumes instantaneous homogeneous mixing whenever new content is injected in the system and therefore provides the maximum mixedness condition. The governing equation is presented in Eq. (6). The convection and diffusion term in the PBE are replaced with a single transport term that is characterised by the mean residence time. This is solved as a global approach with our uncoupled standalone version CPMOD.

$$\frac{\partial n_j}{\partial \mathrm{t}} = B_0 \delta(V - V_{nuc}) - \frac{\partial G \cdot n_j}{\partial V} + \frac{\sum n_{j,in} - n_{j,out}}{\tau_R} \tag{6}$$

Precipitation Kinetics

Supersaturation, which depends on the ion concentration, is a measure of the chemical potential offset from the equilibrium state and is the driving force of the process. In this work, the activity-based supersaturation as defined in Eq. (7) is used because of the high ionic strength (Vicum, et al., 2003). The mean activity coefficients are calculated with the modified Debye-Hückel method by Bromley (1973).

$$S = \gamma_{\pm}\sqrt{\frac{C_{Ba^{2+}}\, C_{SO4^{2-}}}{K_{SP}}} \tag{7}$$

The nucleation and growth rate in Eq. (4) are non-linear to the supersaturation and can be expressed in semi-empirical relations. The kinetics is directly employed from literature since the precipitation kinetics for BaSO4 is well documented. We used the same kinetics expressions, which originate from Mersmann (2001), as in the simulation by Schwarzer, et al (2006). The non-linearity of the kinetics is shown in Figure 2. In the current kinetics model, mono-modal nucleation is assumed. As illustrated, the nucleation rate, nuclei size, as well as the growth rate are very sensitive to the supersaturation. The growth rate, is inversely proportional to the particle size, giving different kinetics in each size interval.

Since the kinetics for each size interval varies, the contribution from each mechanism cannot be directly compared. We can instead characterise the contribution from each mechanism with their timescales. The nucleation and growth timescales are defined in Eq. (8) and Eq. (9) respectively (Baldyga & Bourne, 1999). The smaller the timescale, the stronger the contribution to the process at the instance. By comparing the timescales, the relative proportion of material that is consumed by each mechanism can be identified.

$$\tau_{\mathrm{nuc}} = \frac{\int n(L)dL}{R_n} \tag{8}$$

$$\tau_{\mathrm{G}} = \frac{k_v \int L^3 n(L)dL}{k_a \int G(L)L^2 n(L)dL} \tag{9}$$

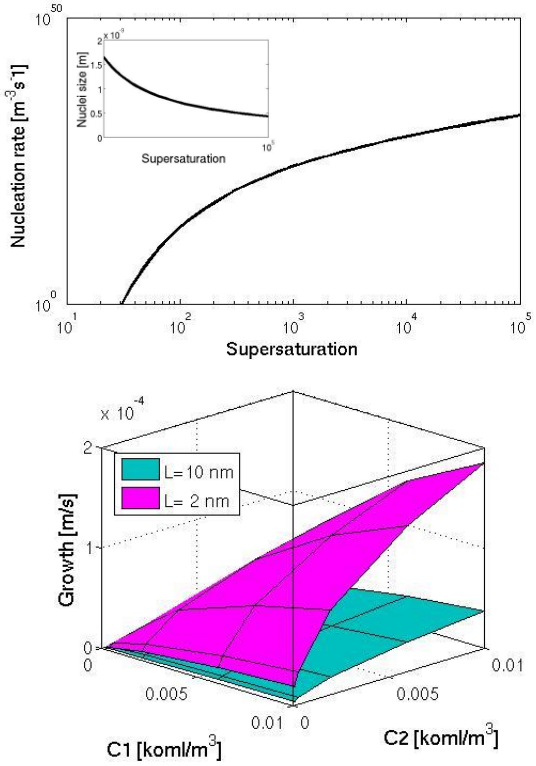

Figure 2. Relation between the supersaturation and concentration composition to the precipitation kinetics. Top: Nucleation rate ; Bottom: Growth rate

RESULTS AND DISCUSSIONS

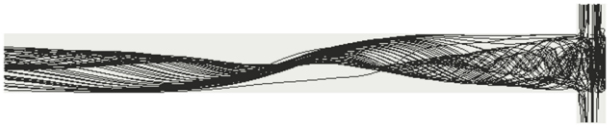

Figure 3. Streamlines in statistically independent state

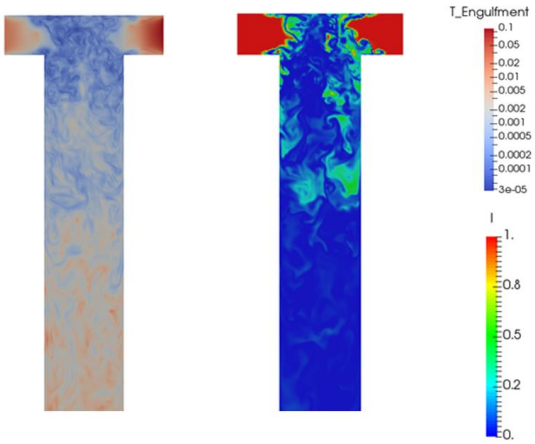

Figure 4. Engulfment mixing timescale (Left) and intensity of seggregation (Right) distribution in the mid-plane of the T-mixer

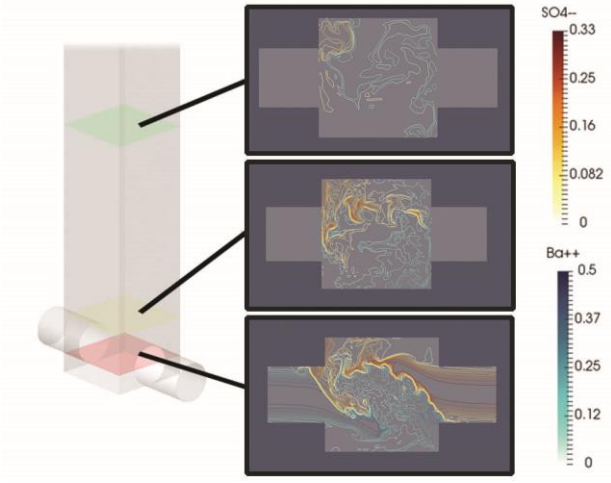

Figure 5. Ion concentration contour along the mixing channel

Flow Field and Mixing

The flow field in the T-mixer is computed with DNS. The Reynolds number, where the characteristic length is defined as the mixing channel width, is 1135. It should be noticed that the flow in T-mixer becomes turbulent at Reynolds number above 400 (Telib, et al., 2004). Figure 3 shows the mean flow streamlines at statistically steady state. The two impinging streams generate a global helical vortex in the mixing channel, providing a global mixing environment. This global vortex introduces turbulence and enhances mixing by breaking down into smaller vortices.

Figure 4 illustrates the distribution of the intensity of segregation and the engulfment timescale in the T-mixer. The intensity of segregation is a measure of the concentration variance and therefore quantify the mixing of a passive scalar

without consumption. On the other hand, the engulfment timescale characterises the timescales of the most energetic vortex in the spectrum (Baldyga & Bourne, 1999). It is computed from the local energy dissipation and is used as a mixing timescale. From the figure, it is shown that the passive scalar is macroscopically mixed very soon after the impingement. This observation indicates that mixing is mostly occurred in the early section of the mixing channel and is confirmed by the mixing time scale distribution: small timescales are localised in the impingement zone.

Figure 5 shows the ion concentration contours in the mixing channel during the precipitation process. In the upstream, when the two species meet in the impingement, sharp boundaries between them are formed and particle formation only take place at these boundaries. The reaction and precipitation in this stage is highly non-uniform. As the species are advected downstream, concentration reduces because of the consumption. The distribution of the ion concentration, and therefore the precipitation process, also becomes more uniform since the mixing evens out spatial differences.

DNS-PBE approach

With the access to the detailed information on the ion concentration, it is now possible to investigate the precipitation process at high resolution. Figure 6 illustrates the supersaturation as well as the corresponding precipitation timescales distribution in the beginning of the process at approximately a quarter of the flow through time after the start of the reaction-precipitation process. The supersaturation field pattern observed in the mid-plane along the mixing channel suggests the build-up of supersaturation follows the helical structure due to the global mixing environment for the ions. High supersaturation spots are concentrated in the most intense mixing region. This is as expected because the blending of reactant increases the total contact area between the species. Since supersaturation is the driving force of nucleation and growth, the precipitation timescales also follow similar pattern and distribution as in supersaturation. In the most intense mixing area, precipitation timescales match with the mixing timescale presented in Figure 5. This indicates the hydrodynamics do influence the precipitation process and therefore the development of the PSD.

Further insights on the contribution on consumption of each mechanism can be obtained from the timescale distribution. Notice that strong nucleation effects are localised in intense mixing area while the effects from growth spread wider in the domain. This implies locally dominating mechanism exists during the process owing to the non-linearity of the kinetics that causes the differences in the contribution from each mechanism. From the results, it is concluded that nucleation dominates high supersaturation regions where mixing is intense whereas growth dominates low supersaturation zones. At intermediate supersaturation, both mechanisms become equally important as there is competition between them. Thus, these results suggest that most of the particles are formed in the impingement zone, the role of the downstream of the mixing channel is to reduce the spatial variance.

Having captured the temporal and spatial evolution of all the local information in the process at high resolution, the coupling is considered successful. It should be noted that this is a general approach for simulating particulate process though it is demonstrated only on $BaSO_4$ precipitation in the present work. It is possible and easy to be applied on other particulate processes as long as the kinetics model is known.

Particle Size Distribution

Figure 7 shows the local PSD at selected spots in the impingement region and along the centreline of the mixing channel respectively together with their neighbouring supersaturation field. It can be immediately observed that the PSD at every point in the domain is different due to the non-uniform consumption from two precipitation mechanisms. The effects of local dominating mechanism are reflected on the local PSD in the formation zone (i.e. the impingement region) as presented. Four different characteristics on the PSD can be identified, and they are correlated with certain states:

1) At spots where nucleation is dominating (for instance, point 1), distribution is biased on the small intervals. The number of particles in the small scales is significantly higher even though the distribution also spread over larger scales due to high supersaturation.
2) At spots where growth is dominating (for instance, point 3), a bell shape distribution is observed. Due to the size dependent kinetics, the particles at small scales grow at a faster rate than the larger scale, resulting in a few small particles in the distribution.
3) At spots where the consumption in nucleation is competing with that in growth (for instance, point 4), both the nucleation and growth dominate characteristics can be identified in the distribution. It is because the precipitation effects (the total volume increase in the product) due to both mechanisms are very close at intermediate supersaturation.
4) At spots where the supersaturation is very low (for instance, point 2), the precipitation effects from both mechanisms become insignificant. The PSD in these spots is therefore negligible.

Downstream, as the ion concentration and supersaturation decays along the mixing channel, the process becomes growth dominated. This effect is shown in Figure 8 that the 0^{th} moment of the distribution (local number of particles) reduce downstream. As aggregation is suppressed in the system, transport is the only mechanism that could lead to reduction of particle number. This indicates that precipitated particles, which are intensely formed in the impingement zone, spread around to the neighbour. The mixing in the channel promote reduction in the spatial variation and even out the PSD, as in the case in the concentration variance.

In Figure 9, the PSD predicted by the PSR case is plotted together with the local PSD. By comparing the local PSD with the PSR solution, it is immediately noticed that PSR predicts smaller particles. Such distribution is caused by the instantaneous mixing in a homogeneous reactor: reaction between high concentration ions is prohibited as the high concentration ions are diluted instantly. As such, high supersaturation, and thus strong precipitation kinetics, could not build up in the reactor. As the maximum mixedness condition imposes a limit to the system, it can therefore be concluded that mixing controls the distribution in a way that the mean particle size can be increased by reducing the mixing intensity so as to limit the consumption in nucleation.

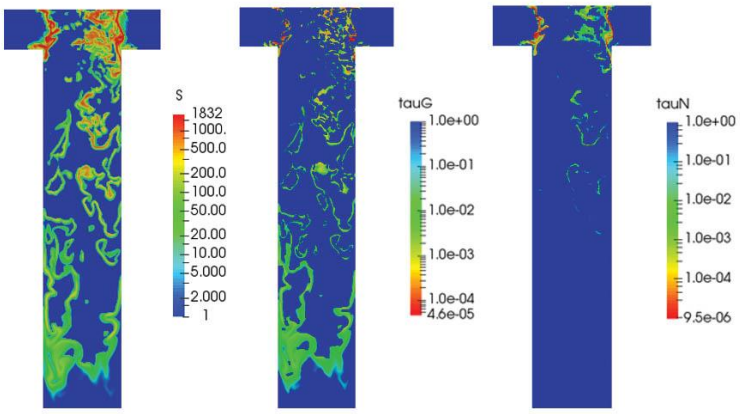

Figure 6. Supersaturation field (Left) in the mid-plane of the T-mixer with the corresponding precipitation timescales of growth (Middle) and nucleation (Right) mechanism

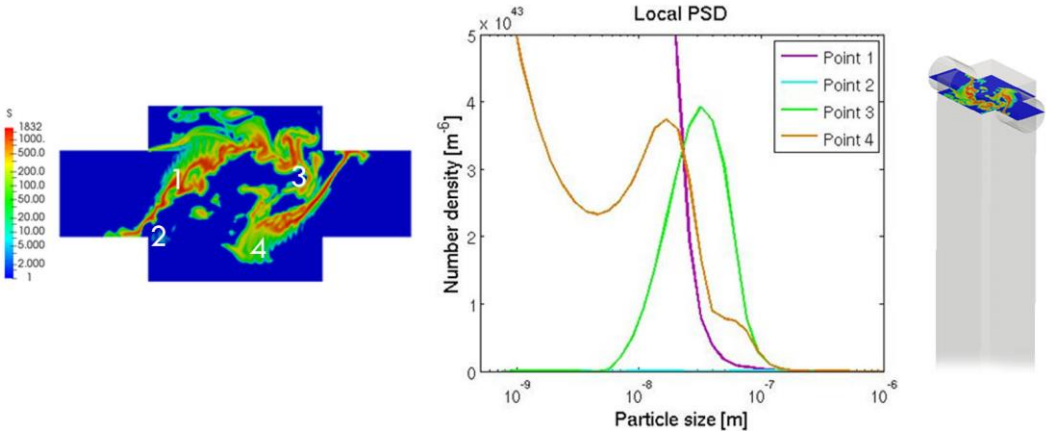

Figure 7. Local PSD at selected location in the impingement zone

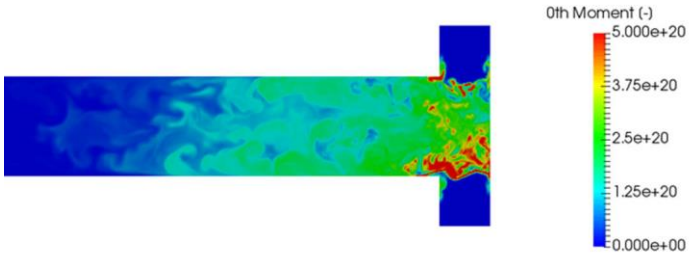

Figure 8. Zeroth moment (total number of particles) distribution

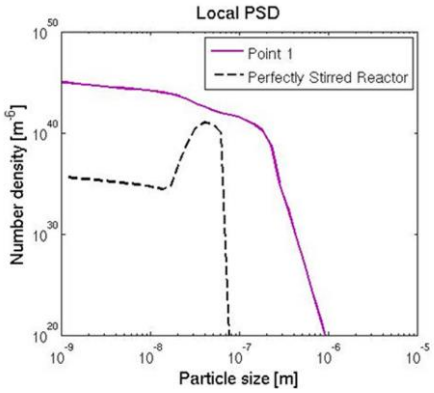

Figure 9. Comparison between the local PSD at point 1 and PSR results. Both axis are in logrithmic scale.

CONCLUSION

A DNS-PBE approach is proposed for simulating and predicting the product PSD in a particulate process in turbulent flow. DNS and PBE were successfully coupled. The application of such approach is demonstrated on a nanoparticle precipitation process in a T-mixer. Thanks to the high spatial and temporal resolution of the supersaturation and species concentration fields, the local kinetics has been successfully captured. This leaded to the investigation on how these local effects affect the consumption and particle formation.

In the context of precipitation in a T-mixer, the proportion of the consumption in nucleation and growth is mostly determined by the mixing intensity around the impingement zone. This leads to different locally dominating mechanisms in the reactor. It is found that most of the particle formation occurs in the impingement zone at spots with high supersaturation whereas the mixing channel evens out the spatial differences. Comparing the PSD with the PSR case, it is shown that the distribution can be controlled by altering the mixing environment.

The local effects on the transient state are observed in the current work. The mixing influences on the final product PSD at the outlet, however, are not yet understood. The effects of the mixing to the process at steady state as well as the correlations between the fluctuations of the hydrodynamics and the precipitation will therefore be investigated in the future works.

NOMENCLATURE

B_0	Nucleation birth term	$m^{-6}\ s^{-1}$
C_i	Molar concentration	$mol\ m^{-3}$
G	Growth rate	$m\ s^{-1}$
k_a	Surface shape factor	-
k_v	Volume shape factor	-
K_{sp}	Solubility Product	$mol^3\ m^{-6}$
L	Particle size	m
M_w	Particle molecular weight	$g\ mol^{-1}$
n_i	Number density of interval i	m^{-6}
r_i	Reaction source term of the i^{th} species	$mol\ m^{-3}\ s^{-1}$
R_n	Nucleation rate	$m^{-3}\ s^{-1}$
S	Supersaturation	-
St	Schmidt number	-
t	Time	s
u	Velocity	$m\ s^{-1}$
V	Particle size	m^3
$V_{m,i}$	Midpoint of size interval i	m^3

Greek letter

$\gamma_\pm$	Activity coefficient	-
τ	timescales	s
τ_R	Residence time	s
ρ	Particle density	$kg\ m^{-3}$
μ	Mixture viscosity	$Pa\ s$

Subscript

in	Inlet
out	Outlet
nuc	Nucleation
G	growth

REFERENCES

Baldyga, J. & Bourne, J., 1999. *Turbulent mixing and chemical reaction.* Chichester: Wiley.

Bromley, L., 1973. Thermodynamic properties of strong electrolytes in aqueous solutions. *AlChE J.,* Volume 19, pp. 313-320.

Fishpool, G. & Leschziner, M., 2009. Stability bounds for explicit fractional-step schemes for the Navier-Stokes equations at high Reynolds number. *Computer & Fluids,* Volume 38, pp. 1289-1298.

Gradl, J., Schwarzer, H., Schwertfirm, F., Manhart, M., Peukert, W., 2006. Precipitation of nanoparticles in a T-mixer: Coupling the particle population dynamics with hydrodynamics through direct numerical simulation. *Chemical Engineering and Processing,* Volume 45, pp. 908-916.

Immanuvel, P., Papadakis, G. & Vassilicos, J., 2017. Genesis and evolution of velocity gradients in near-field spatially developing turbulence. *Journal of Fluid Mechanics,* Volume 815, pp. 295-332.

Mersmannm, A., 2001. *Crystallization Technology Handbook.* 2 ed. New York: Marcel Dekker.

Metzger, L. & Kind, M., 2017. The influence of mixing on fast precipitation processes - A coupled 3D CFD-PBE approach using the direct quadrature method of moments (DQMOM). *Chem. Eng. Sci.,* Volume 169, pp. 284-298.

Qamar, S., Elsner, M.P., Angelov, I.A., Warnecke, G. & Seidel-Morgenstern, A., 2006. A comparative study of high resolution schemes for solving population balance in crystallization. *Computers and Chemical Engineering,* pp. 1119-1131.

Rigopoulos, S. & Jones, A., 2003. Finite-element scheme for solution of the dynamic population balance equation. *AlChE Journal,* 49(5), pp. 1127-1139.

Schwarzer, H. & Peukert, W., 2004a. Combined experimental / numerical study on the precipitation of nanoparticles. *AIChE J.,* Volume 50, pp. 3234-3247.

Schwarzer, H. & Peukert, W., 2004b. Tailoring particle size though nanoparticle precipitation. *Chem. Eng. Comm.,* Volume 191, pp. 580-606.

Schwarzer, H., Schwertfirm, F., Manhart, M., Schmid, H., Peukert, W., 2006. Predictive simulation of nanoparticle precipitation based on the population balance equation. *Chemical Engineering Science,* Volume 61, pp. 167-181.

Sewerin, F. & Rigopoulos, S., 2017. An LES_PBE-PDF approach for modelling particle formation in turbulent flows. *Physics of Fluids.*

Telib, H., Manhart, M. & Iollo, A., 2004. Analysis and low-order modelling of the inhomogeneous transitional flow inside a T-mixer. *Physics of Fluids,* Volume 16, pp. 2717-2731.

Vicum, L., Mazzotti, M. & Baldyga, J., 2003. Applying a thermodynamic model to the non-stoichiometric precipoitation of Barium Sulfate. *Chem. Eng. Technol.,* pp. 325-333.

ACKONWLEDGEMENT

This work used the ARCHER UK National Supercomputer Service (http://www.archer.ac.uk) and was supported by the UK Consortium on Turbulent Reacting Flows [EP/K026801/1].

The authors acknowledge the IChemE's Fluid Mixing Processes Special Interest Group and Syngenta for their generous financial support.